

Resonant Raman Scattering by Elementary Electronic Excitations in Semiconductor Structures

S. Das Sarma and Daw-Wei Wang

Department of Physics, University of Maryland, College Park, Maryland 20742-4111

(Received 5 January 1999)

We explain quantitatively why resonant Raman scattering spectroscopy, an extensively used experimental tool in studying elementary electronic excitations in doped low-dimensional semiconductor nanostructures, always produces an observable peak at the so-called “single particle” excitation although the standard theory predicts that there should be no such single particle peak in the Raman spectra. We have thus resolved an experimental puzzle which dates back more than 25 years.

PACS numbers: 73.20.Mf, 71.45.-d, 78.30.Fs

Resonant Raman scattering (RRS) involving inelastic scattering of light by electrons has long been a powerful and versatile spectroscopic tool for studying [1–10] elementary excitations in doped low-dimensional semiconductor structures such as quantum wells, superlattices, and, more recently, one-dimensional quantum wire systems. RRS has been extensively used in experimentally studying the collective charge density excitation (CDE) dispersion in semiconductor quantum wells, quantum wires, and superlattices for both intrasubband and intersubband transitions. In the standard theory [11,12], which ignores the role of the valence band and simplistically assumes the photon to be interacting entirely with conduction band electrons, RRS intensity is proportional to the dynamical structure factor [13] of the conduction band electron system and therefore has peaks at the collective mode frequencies at the appropriate wave vectors defined by the experimental geometry. Restricting to the polarized RRS geometry [12], where the incident and scattered photons have the same polarization vectors indicating the absence of spin flips in the electronic excitations, the dynamical structure factor peaks should correspond to the poles of the reducible density response function, which are given by the collective CDEs of the system. In particular, the single particle electron-hole excitations (SPE), which are at the poles of the corresponding irreducible response function, carry no long wavelength spectral weight in the density response function and should *not*, as a matter of principle, show up in the polarized RRS spectra. The remarkable experimental fact, however, is that there is always a relatively weak (but quite distinct) low energy SPE peak in the observed RRS spectra (near resonance) in addition to the expected strong CDE peak at higher energy. This observed SPE peak in the polarized RRS spectra is a factor of 10^3 – 10^4 times stronger than that given by the calculated dynamical structure factor in the standard theory. This puzzling feature of an ubiquitous anomalous SPE peak (in addition to the expected CDE peak) in the observed RRS spectra occurs in one-dimensional GaAs-AlGaAs quantum wires, two-dimensional GaAs quantum wells, and even in the doped three-dimensional bulk GaAs systems [1]. It exists in

the low-dimensional structures both for intrasubband and intersubband (i.e., transitions along and perpendicular to the confining quantization direction) excitations, and in zero and finite magnetic fields. No theoretical understanding of this phenomenon exists in spite of the great ubiquitousness of the effect. *Ad hoc* proposals [2,14] have been made in the literature that perhaps a serious breakdown of momentum or wave vector conservation (arising, for example, from scattering by random impurities) is responsible for somehow transferring spectral weight from large to small wave vectors. Apart from being completely *ad hoc*, this proposal also suffers from any lack of empirical evidence in its support—in particular, the observed anomalous SPE peak in the RRS spectra does not correlate with the strength of the impurity scattering in the system. The ubiquitousness of the phenomenon suggests that it must arise from some generic principle underlying RRS itself, and cannot be explained by nongeneric and manifestly system-specific proposals which have been made occasionally in the literature. We emphasize that this very basic lack of understanding of why an SPE peak shows up in the experimental RRS spectra of doped semiconductor structures is an important problem because the RRS is one of the most powerful techniques to study an interacting electron system in one, two, and three dimensions, including even quantum Hall systems.

In this Letter we provide a quantitative and *compellingly generic* theoretical explanation for this puzzle. We emphasize that the generic nature of the phenomenon strongly suggests that its quantitative explanation must lie in the fundamental principles of RRS and must not depend on the experimental details [1–10], such as the system dimensionality, intrasubband or intersubband excitations being probed, the existence (or not) of an external magnetic field, etc. Our theory depends only on the resonant nature [12,15–17] of the experiment (i.e., the laser frequency of the external light used in the RRS is approximately equal to the fundamental band gap of the semiconductor, which causes a resonant enhancement of the RRS intensity allowing the observation of the elementary electronic excitations in the conduction band which usually do not couple to light).

In Fig. 1(a) we depict the schematic diagram [15–17] for the two step process (steps 1 and 2 in the figure) involved in the polarized RRS spectroscopy at the $E_0 + \Delta_0$ direct gap of GaAs [17] where an electron in the valence band is excited by the incident photon into an excited (i.e., above the Fermi level) conduction band state, leaving a valence band hole behind (step 1); then an electron from inside the conduction band Fermi surface combines with the hole in the valence band (step 2). Electron spin is conserved throughout the scattering process. In the standard random phase approximation (RPA), which neglects all interband resonance effects and considers only the conduction band, the RRS intensity will then be proportional [11] to the imaginary part of the reducible response function, which is given by $-\text{Im}\Pi(\mathbf{q}, \omega)$, where $\Pi(\mathbf{q}, \omega) = \Pi^{(0)}(\mathbf{q}, \omega) \epsilon(\mathbf{q}, \omega)^{-1}$ is the reducible polarizability with $\Pi^{(0)}(\mathbf{q}, \omega)$ as the noninteracting conduction band electron polarizability and $\epsilon(\mathbf{q}, \omega) = 1 - v_c(\mathbf{q}) \Pi^{(0)}(\mathbf{q}, \omega)$ is the appropriate dynamical dielectric function [with $v_c(\mathbf{q})$ as the Coulomb interaction]—the geometric series of “bubble” diagrams in Fig. 1(c) is the characteristic feature of a CDE or a plasmon excitation. We show in Fig. 2 some typical calculated one-dimensional (1D) RRS spectra based on this simple formula which has been universally employed [11] in the literature. The calculated spectrum gives reasonable quantitative agreement with the experimentally observed [6] polarized RRS spectra for the CDE peak in 1D GaAs quantum wires (the same is true in higher dimensions—see, for example, Ref. [11]) except for one important feature—the theoretical spectrum has only one peak corresponding to the CDE, whereas experimentally one always sees an SPE peak at resonance.

We now consider the full resonance situation including the valence band which obviously [12,15–18] plays a crucial role in the RRS experiment because the external photon energy must approximately equal the $E_0 + \Delta_0$ direct gap for the experiment to succeed. We can write (assuming the usual $\mathbf{p} \cdot \mathbf{A}$ coupling of light to matter) the RRS scattering cross section [17] for the resonant scattering process for the conduction band electrons as

$$\gamma(\mathbf{k}) = \hat{n}_i \cdot \hat{n}_f + \frac{1}{m_c} \left(\frac{c\langle \mathbf{k} | \hat{n}_f \cdot \mathbf{p} | \mathbf{k} + \mathbf{k}_f \rangle_v \langle \mathbf{k} + \mathbf{k}_f | \hat{n}_i \cdot \mathbf{p} | \mathbf{k} - \mathbf{q} \rangle_c}{E_g + E_c(\mathbf{k}) - E_v(\mathbf{k} + \mathbf{k}_f) + \omega_i} + \frac{c\langle \mathbf{k} | \hat{n}_i \cdot \mathbf{p} | \mathbf{k} - \mathbf{k}_i \rangle_v \langle \mathbf{k} - \mathbf{k}_i | \hat{n}_f \cdot \mathbf{p} | \mathbf{k} - \mathbf{q} \rangle_c}{E_g + E_c(\mathbf{k}) - E_v(\mathbf{k} - \mathbf{k}_i) - \omega_i} \right), \quad (3)$$

where $c_{\mathbf{k}}$'s are fermion operators of wave vector \mathbf{k} and the spin index is neglected; \hat{n}_i/\hat{n}_f , $\mathbf{k}_i/\mathbf{k}_f$, and ω_i/ω_f are, respectively, the initial/final photon polarization vectors, wave vectors, and frequencies; $|\mathbf{k}\rangle_{c,v}$ and $E_{c,v}(\mathbf{k})$ refer to conduction/valence band Bloch states and energies for a wave vector \mathbf{k} in the corresponding band; $\omega \equiv \omega_i - \omega_f$, $\mathbf{q} \equiv \mathbf{k}_i - \mathbf{k}_f$ are the energy and wave vector difference

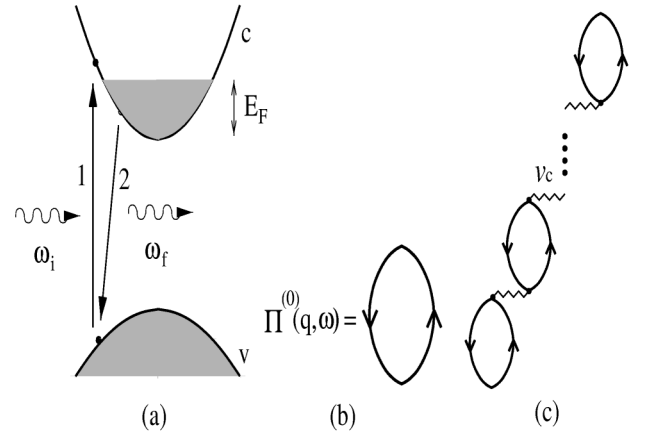


FIG. 1. (a) Schematic representation of the resonant Raman scattering in the doped, direct gap two band model of GaAs nanostructure. ω_i and ω_f are the initial and final frequencies of the external photon. Steps 1 and 2 are described in the text. The RRS is a two step process that involves steps 1 and 2, leaving an excited electron-hole pair in the conduction band. (b) Diagrammatic representation of the conduction band irreducible polarizability, $\Pi^{(0)}(\mathbf{q}, \omega)$, in RPA calculation. (c) Diagrammatic representation of the conduction band reducible polarizability, $\Pi(\mathbf{q}, \omega)$, in the standard theory. $v_c(\mathbf{q})$ is the Coulomb interaction.

(using i, f to denote the initial prescattering and the final postscattering states)

$$\frac{d^2\sigma}{d\Omega d\omega} \propto \frac{\omega_f}{\omega_i} \langle \sum_F |M_{FI}|^2 \delta(E_F - E_I - \omega) \rangle_I, \quad (1)$$

where ω_f , ω_i are the final and initial photon energies, and ω is their difference [$\hbar = 1$ and a sum over all final electronic states, F , and an average over all initial electronic states, I , are implied in Eq. (1)]. M_{FI} is the transition matrix element defined by (using the subscripts c and v to denote the conduction and valence band electronic Bloch states, respectively, in our two band model) [19]

$$M_{FI} = \langle F | \sum_{\mathbf{k}} \gamma(\mathbf{k}) c_{\mathbf{k}}^\dagger c_{\mathbf{k}-\mathbf{q}} | I \rangle, \quad (2)$$

of the photons in the experiment. Assuming the resonance condition, i.e., $\omega_i \approx E_g + E_c(k_F) - E_v(k_F)$, where E_g is the $E_0 + \Delta_0$ band gap and k_F is the Fermi wave vector in the conduction band, the usual backscattering experimental geometry, i.e., $\mathbf{q} = 2\mathbf{k}_i$, and the well-satisfied condition $|\mathbf{k}_i| \sim |\mathbf{k}_f| \ll k_F$ due to the long wavelength ($\sim 5000 \text{ \AA}$) of visible light compared with the Fermi

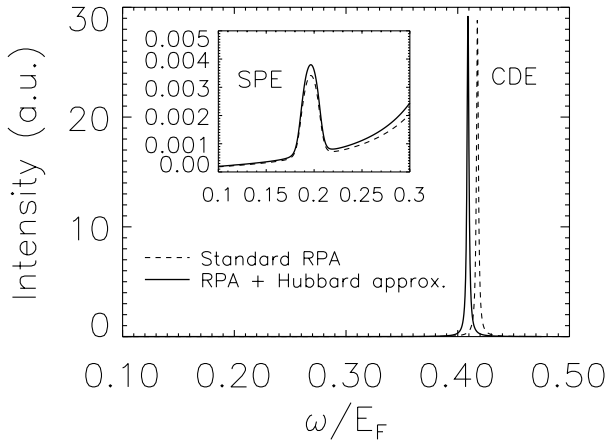


FIG. 2. The dynamical structure factor in the standard theory for 1D quantum wire system calculated by RPA in long wavelength limit ($q = 0.1k_F$). Vertex correction by Hubbard approximation is also shown for comparison. The SPE peak (inset) is much smaller ($\sim 10^{-4}$) than the CDE peak in the standard theory. Finite impurity scattering effect (included in the theory) leads to the broadening of the peaks.

wavelength ($\sim 100 \text{ \AA}$ or less), Eqs. (1) and (2) can be written as

$$\frac{d^2\sigma}{d\Omega d\omega} \sim -\text{Im} \left[\Pi^{(2)}(\mathbf{q}, \omega) + \frac{[\Pi^{(1)}(\mathbf{q}, \omega)]^2 v_c(\mathbf{q})}{\epsilon(\mathbf{q}, \omega)} \right], \quad (4)$$

where

$$\begin{aligned} \Pi^{(n)}(\mathbf{q}, \omega) &= \frac{-2}{(2\pi)^D} \int d^D p \\ &\times \frac{[A(\mathbf{p}, \mathbf{q})]^n [n_c(\mathbf{p}) - n_c(\mathbf{p} - \mathbf{q})]}{\omega + i\delta - E_c(\mathbf{p}) + E_c(\mathbf{p} - \mathbf{q})}, \end{aligned} \quad (5)$$

where D is the dimensionality, and $n_c(\mathbf{p})$ refers to the conduction band Fermi occupancy for wave vector \mathbf{p} with

$$\begin{aligned} A(\mathbf{p}, \mathbf{q}) &= [E_\omega + (1 + \xi)(\tilde{\mathbf{p}}^2 - 1) \\ &+ \xi(-\tilde{\mathbf{p}} \cdot \tilde{\mathbf{q}} + \tilde{\mathbf{q}}^2/4)]^{-1}, \end{aligned} \quad (6)$$

where $E_\omega \equiv E_F^{-1}[E_g + (1 + \xi)k_F^2/2m_c - \omega_i]$; $\xi \equiv m_c/m_v$; $\tilde{\mathbf{p}} \equiv \mathbf{p}/k_F$; $\tilde{\mathbf{q}} \equiv \mathbf{q}/k_F$; and $E_F = E_c(k_F)$ is the Fermi energy of the conduction band electrons. We have assumed parabolic band dispersions near the band extrema with m_c and m_v as the conduction and valence band effective masses. Using GaAs band parameters we can now calculate the polarized RRS spectra from Eq. (3). Note that the resonance effects are nonperturbative and depend crucially on the exact value of the incident photon energy. Our theory can be considered to be a *resonant* RPA theory which explicitly takes into account the interband resonant process involved in the RRS experiments.

In Figs. 3–5 we give our representative results for the calculated polarized RRS spectra for intrasubband ele-

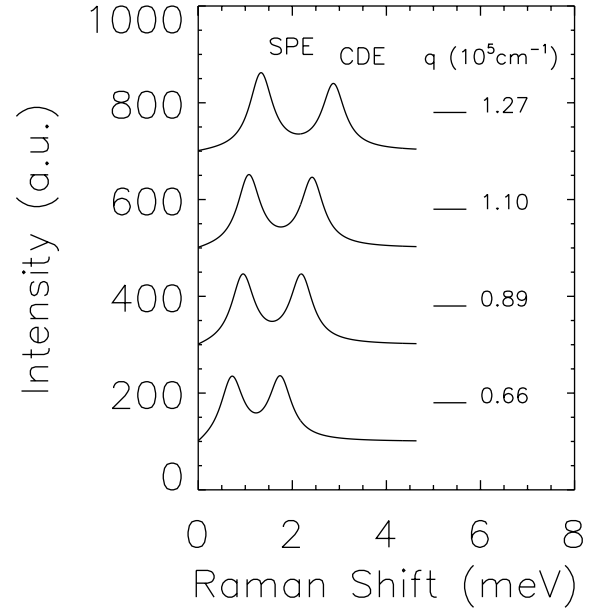


FIG. 3. The calculated resonant Raman scattering intensity in the full theory including the interband transition for a realistic 1D quantum wire system. The SPE spectral weight is enhanced by the resonance and is now comparable to that of CDE. The parameters are chosen to correspond to the experimental system of Ref. [6], where the resonance condition is satisfied. Our theoretical results agree very well with the experimental data shown in the Fig. 1 of Ref. [6].

mentary excitations for GaAs 1D and 2D structures. In Fig. 3 the specific wave vectors and other system details have been chosen for the experimental GaAs quantum wires of Ref. [6]. Our calculated spectra at resonance are in quantitative agreement with the corresponding experimental RRS spectra shown in Fig. 1 of Ref. [6]. The calculated SPE spectral weight at resonance in our Fig. 3

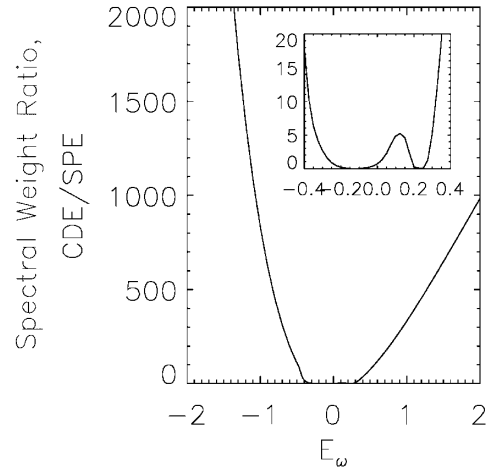


FIG. 4. The resonant Raman scattering spectral weight ratio of CDE to SPE as a function of the resonance parameter, E_ω . For off-resonance, $|E_\omega| \geq 0.5$, CDE always dominates SPE, but within the resonance region, $|E_\omega| < 0.5$, the SPE could be stronger than CDE as shown in the inset. All parameters are the same as those in Fig. 3.

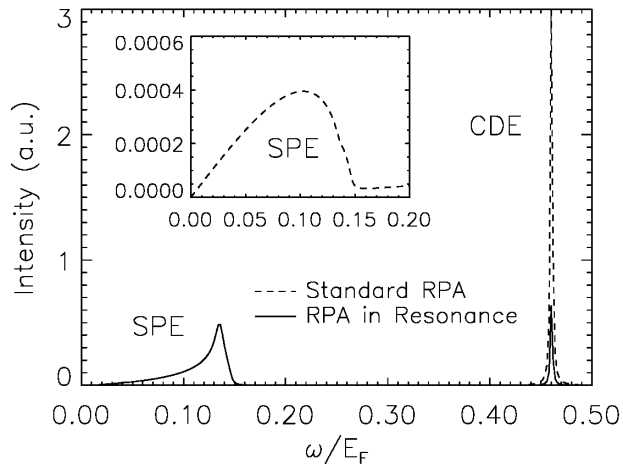


FIG. 5. The calculated 2D resonant Raman scattering intensity in the full theory in the long wavelength limit ($q = 0.1k_F$). Simple RPA result in the standard theory is also shown for comparison. The resonance effect ($E_\omega = 0.23$) strongly enhances SPE and suppresses CDE in the 2D system similar to the 1D system. The inset shows the very weak SPE peak in the standard theory, which should be manifestly experimentally unobservable.

is comparable to that of the CDE (to be contrasted with the simple nonresonant calculation shown in Fig. 2). We emphasize that this spectacular enhancement of SPE spectral weight in the resonant scattering process disappears as one moves away from resonance. This can be seen in Fig. 4, where we plot the spectral weight ratio of CDE/SPE weight as a function of the resonance condition itself. It is obvious that the SPE spectral weight, while having a rather nontrivial structure around the resonance condition, is essentially zero far away from resonance where the CDE dominates. Experimentally it is well known that the SPE spectral weight dies off as the incident photon energy goes off-resonance. Our detailed theoretical results provide specific nontrivial predictions about how the SPE spectral weight should vary as a function of the incident photon energy. Finally in Fig. 5 we show some representative calculations for 2D polarized RRS spectra (as appropriate for elementary conduction band excitations in GaAs quantum wells) in 2D systems. While the quantitative details for the 2D systems differ from the corresponding 1D results, the basic theoretical phenomenon is the same: the SPE spectral weight is anomalously enhanced at resonance compared with the simple RPA, whereas off-resonance the SPE spectral weight decreases, eventually becoming negligibly small.

As a concluding note it may be important to emphasize that the nomenclature “SPE” peak, which we have used throughout this paper following the standard experimental

literature [1–10], characterizing the low energy RRS peak is inappropriate since the SPE strictly corresponds to a peak in $\text{Im}\Pi^{(0)}$. We also note that interaction effects have been neglected in our irreducible response function in the spirit of RPA, which is entirely justifiable in two and three dimensions, but is open to question in 1D. We are currently [20] investigating 1D interaction effects on the RRS spectra by going beyond the resonant RPA scheme of Eqs. (1)–(6)—we find that perturbative or mean-field (e.g., Hubbard approximation) inclusion of interaction effects does not qualitatively affect the RPA results. The striking phenomenological similarity in the experimentally observed RRS spectra in one-, two-, and three-dimensional systems is a strong indication that generic resonance physics as studied in this paper (within a *resonant* RPA scheme) is playing a fundamental role in producing the low energy SPE feature in the polarized RRS spectra.

We thank A.J. Millis for critical discussions, and the US-ONR and the US-ARO for support.

-
- [1] A. Pinczuk *et al.*, Phys. Rev. Lett. **27**, 317 (1971).
 - [2] A. Pinczuk *et al.*, Phys. Rev. Lett. **61**, 2701 (1988).
 - [3] A. Pinczuk *et al.*, Phys. Rev. Lett. **63**, 1633 (1989).
 - [4] D. Gammon *et al.*, Phys. Rev. B **41**, 12311 (1990); M. Berz *et al.*, Phys. Rev. B **42**, 11957 (1990).
 - [5] A. Pinczuk *et al.*, Phys. Rev. Lett. **70**, 3983 (1993).
 - [6] A. R. Goñi *et al.*, Phys. Rev. Lett. **67**, 3298 (1991).
 - [7] D. Gammon *et al.*, Phys. Rev. Lett. **68**, 1884 (1992); R. Decca *et al.*, Phys. Rev. Lett. **72**, 1506 (1994).
 - [8] A. Schmeller *et al.*, Phys. Rev. B **49**, 14778 (1994).
 - [9] C. Schüller *et al.*, Phys. Rev. B **54**, R17304 (1996).
 - [10] R. Strenz *et al.*, Phys. Rev. Lett. **73**, 3022 (1994).
 - [11] J. K. Jain and P. B. Allen, Phys. Rev. Lett. **54**, 947 (1985); Phys. Rev. Lett. **54**, 2437 (1985); S. Das Sarma and E. H. Hwang, Phys. Rev. Lett. **81**, 4216 (1998).
 - [12] A. Pinczuk *et al.*, Philos. Mag. B **70**, 429 (1994), and references therein.
 - [13] D. Pines, *The Theory of Quantum Liquids* (Benjamin, New York, 1966).
 - [14] I. K. Marmorosk and S. Das Sarma, Phys. Rev. B **45**, 13396 (1992).
 - [15] M. V. Klein, in *Light Scattering in Solids*, edited by M. Cardona (Springer-Verlag, New York, 1975), p. 147.
 - [16] E. Burstein *et al.*, Surf. Sci. **98**, 451 (1980).
 - [17] A. Pinczuk and G. Abstreiter, in *Light Scattering in Solids V*, edited by M. Cardona and G. Güntherodt (Springer-Verlag, New York, 1989), p. 153.
 - [18] P. A. Wolff, Phys. Rev. **171**, 436 (1968); F. A. Blum, Phys. Rev. B **1**, 1125 (1970).
 - [19] P. A. Wolff, Phys. Rev. Lett. **16**, 225 (1966).
 - [20] D. W. Wang, A. J. Millis, and S. Das Sarma (unpublished).